Analytical Approach to Cogging Torque Calculation of PM Brushless Motors

Jacek F. Gieras, *Fellow, IEEE*

***Abstract*—This paper discusses the approach to analytical calculation of the cogging torque in permanent-magnet (PM) brushless motors. Magnetic field energy in the air gap has been used to obtain the cogging torque equations. Two equations have been derived: with the PM circumferential width taken into account, and a simplified equation, i.e., without the effect of the finite width of the PM. The effect of eccentricity has also been included. Calculation results have been compared with laboratory test results**

***Index Terms*—AC motors, brushless motors, cogging torque, magnetic flux density, permanent-magnet (PM) machines, PM motors, stator slots, torque ripple.**

I. Introduction

THE instantaneous torque of an electrical motor has two components, i.e., constant or average component and periodic component. The periodic component is a function of time or rotor position, superimposed on the constant component. The periodic component causes the *torque pulsation* also called the torque ripple. The *torque ripple* is caused by both the construction of the machine and power supply.

There are three sources of the torque ripple coming from the construction of the magnetic and electric circuit of a machine:

- cogging effect, i.e., interaction between the rotor magnetic flux and variable permeance of the air gap due to the geometry of stator slots;
- distortion of the sinusoidal or trapezoidal distribution of the magnetic flux density in the air gap;
- differences between permeances of the air gap in the d and q axes.

The cogging effect produces the so-called *cogging torque*, higher harmonic of the magnetic flux density in the air gap produce the *field harmonic electromagnetic torque*, and the unequal permeance in the d and q axes produces the *reluctance torque*.

The torque ripple caused by the power supply is due to the current ripple resulting, e.g., from the pulsewidth modulation (PWM) and/or phase current commutation.

The most comprehensive literature review and comparison of methods of the torque ripple reduction is given in [4]. Analytical methods of cogging torque calculation usually neglect the magnetic flux in the stator slots and magnetic saturation of the stator teeth [1]–[3], [5], [6], [12], [13], [15], [16]. Cogging torque is derived from the magnetic flux density distribution either by calculating the rate of change of total energy stored in the air gap with respect to the rotor angular position [1]–[3], [6], [12], [13] or by summing the lateral magnetic forces along the sides of the stator teeth [15]. Many cogging torque calculations are specific to a particular method of reducing the cogging effect [8].

Paper IPCSD-04-029, presented at the 2003 IEEE International Electric Machines and Drives Conference, Madison, WI, June 1–4, and approved for publication in the IEEE TRANSACTIONS ON INDUSTRY APPLICATIONS by the Electric Machines Committee of the IEEE Industry Applications Society. Manuscript submitted for review August 21, 2003 and released for publication May 18, 2004.

The author is with the United Technologies Research Center, East Hartford, CT 06108 USA (e-mail: gierasjf@utrc.utc.com).

Digital Object Identifier 10.1109/TIA.2004.834108

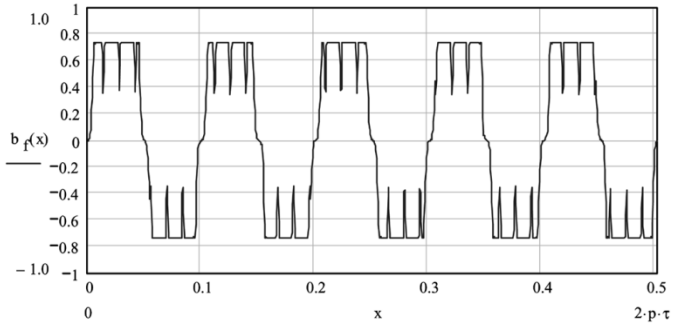

Fig. 1. Distribution of the normal component $b_f(x)$ of the magnetic flux density in the air gap (Tesla versus meter) of a ten-pole, 36-slot PM brushless machine according to (1)–(3).

In this paper a new analytical method of cogging torque calculation of permanent-magnet (PM) brushless motors is discussed. The proposed method uses the energy of magnetic field in the air gap and classical equations for the air-gap magnetic flux density distribution in ac machines with slotted stators [7], [9], [14].

II. Air Gap Magnetic Flux Density

The normal component of the magnetic flux density distribution in the air gap (Fig. 1) of a PM brushless motor with slotted stator core can be expressed as (see Appendix I)

$$b_f(x) = \frac{b_{PM}(x)}{k_C} + b_{sl}(x). \tag{1}$$

The x coordinate is in the direction of rotation. The magnetic flux density component excited by the rotor PMs is a sum of higher space harmonics μ, i.e.,

$$b_{PM}(x) = \sum_{\mu} B_g b_\mu k_{s\mu} \cos\left(\mu \frac{\pi}{\tau} x\right) \tag{2}$$

and the magnetic flux density component due to stator slots is approximated as

$$b_{sl}(x) = -2\gamma \frac{g}{t_1} \sum_{k=1}^{\infty} k_{0k}^2 k_{sk}^2 \cos\left(k \frac{2\pi}{t_1} x\right) \times \sum_{\mu} B_g b_\mu k_{s\mu} \cos\left(\mu \frac{\pi}{\tau} x\right). \tag{3}$$

Equation (3) results from the classical theory of ac electrical machines, e.g., [7], [9], and [14]. In (1)–(3), k_C is Carter's coefficient of the air gap taking into account slot openings (see Appendix I), B_g is the flat-topped value of the periodical magnetic flux density waveform excited in the air gap by the rotor PMs, $k = 1,2,3,\ldots$, $\mu = 6l \pm 1$ are the rotor higher space harmonics where $l = 1,2,3,\ldots$, b_μ is the Fourier coefficient of the magnetic flux density distribution excited by the rotor PMs (see Appendix II), $k_{s\mu}$ is the rotor PM skew factor, τ is the pole pitch, γ is the parameter depending on the slot opening b_{14} and the air gap g (see Appendix I), t_1 is the stator slot pitch, k_{0k} is the stator slot opening factor, and k_{sk} is the stator slot skew factor. In general, both PMs and stator slots can be skewed.

The skew factors and slot opening factor are defined by the following equations:

- the rotor PM skew factor

$$k_{s\mu} = \frac{\sin\left(\mu\pi\frac{b_{fs}}{2\tau}\right)}{\mu\pi\frac{b_{fs}}{2\tau}} \tag{4}$$

- the stator skew factor

$$k_{sk} = \frac{\sin\left(k\pi\frac{b_s}{2t_1}\right)}{k\pi\frac{b_s}{2t_1}} \tag{5}$$

- the stator slot opening factor [14]

$$k_{ok} = \frac{\sin\left(k\rho\pi\frac{b_{14}}{2t_1}\right)}{k\rho\pi\frac{b_{14}}{2t_1}} \tag{6}$$

where [7], [14]

$$\rho = \frac{\frac{b_{14}}{t_1}}{5+\frac{b_{14}}{t_1}}\frac{2\sqrt{1+(\frac{b_{14}}{t_1})^2}}{\sqrt{1+(\frac{b_{14}}{t_1})^2}-1}. \tag{7}$$

The skew of PMs is b_{fs} and the skew of stator slots is b_s. For most PM configurations the air gap g is to be replaced by an equivalent air gap $g' \approx g + h_M/\mu_{\mathrm{rrec}}$ where g is the mechanical clearance, h_M is the radial height of the PM (one pole), and $\mu_{\mathrm{rrec}} = 1.02$–$1.1$ is the relative recoil permeability of the PM material [11].

III. Calculation of Cogging Torque

If the magnetic saturation and armature reaction are negligible, the cogging torque is independent of the stator current. The frequency of the fundamental component of the cogging torque is $f_c = s_1 n_s$, where s_1 is the number of the stator slots and n_s is the rotor speed in revolutions per second.

Assuming that the total energy W of the magnetic field is stored in the air gap, the cogging torque is expressed as

$$T_c(x) = -\frac{dW}{d\theta} = -\frac{D_{2\mathrm{out}}}{2}\frac{dW}{dx} \tag{8}$$

where $D_{2\mathrm{out}} \approx D_{1\mathrm{in}}$ is the rotor outer diameter, $D_{1\mathrm{in}}$ is the stator inner diameter and the x axis is in the direction of rotation. The mechanical angle

$$\theta = \frac{2\pi}{D_{2\mathrm{out}}}. \tag{9}$$

The rate of change of the air-gap coenergy is

$$W(x) = \frac{L_i g}{2\mu_0}\int b_f^2(x)dx \tag{10}$$

where L_i is the effective length of the stator stack, μ_0 is the magnetic permeability of free space, g is the air gap, and $b_f(x)$ is the air-gap magnetic flux density distribution according to (1). Substituting (1) and (10) into (8) and assuming that the maximum energy change is in the interval $X + a \le x \le X + b$, the cogging torque equation becomes

$$T_c(X) = -\frac{L_i g}{2\mu_0}\frac{D_{2\mathrm{out}}}{2}\frac{\partial}{\partial x}\int_{X+a}^{X+b}\left[\frac{b_{PM}(x)}{k_C} + b_{sl}(x)\right]^2 dx. \tag{11}$$

According to [6], the maximum energy change occurs for $a = 0.5t_1$ and $b = 0.5b_{14} + c_t$ where $c_t = t_1 - b_{14}$. Taking into account only fundamental space harmonics $\mu = 1$ and $k = 1$, the expression in the square bracket under the integral will have the following form:

$$\left[\frac{b_{PM}(x)}{k_C} + b_{sl}(x)\right]^2 = \left[\frac{1}{k_C}B\cos\beta x - AB\cos\alpha x\cos\beta x\right]^2 \tag{12}$$

where

$$A = 2\gamma\frac{g}{t_1}k_{ok=1}^2 k_{sk=1}^2 \quad B = B_g b_{\mu=1} k_{s\mu=1} \tag{13}$$

$$\alpha = \frac{2\pi}{t_1} \quad \beta = \frac{\pi}{\tau}. \tag{14}$$

With a stationary stator, only the magnetic flux density excited by the rotor PMs depends on the rotor position with respect to the coordinate system fixed to the stator [14]. Magnetic flux density waveforms are visualized in Fig. 2. It is easier to take the integral over $b_f(x)^2$ assuming that the rotor is stationary and the stator moves with synchronous speed, i.e., only stator slots expressed by the term $A\cos\alpha x$ change their position. Thus,

$$T_c(X) = -\frac{L_i g}{2\mu_0}\frac{D_{2\mathrm{out}}}{2} \times \int_{X+a}^{X+b} 2\left[\frac{1}{k_C}B\cos\beta x - AB\cos\alpha x\cos\beta x\right] \times (-AB\alpha\sin\alpha x\cos\beta x)dx. \tag{15}$$

After performing integration with respect to x the cogging torque equation takes the following form:

$$T_c(X) = -\frac{L_i g}{2\mu_0}\frac{D_{2\mathrm{out}}}{2}\left[I_1(X) + I_2(X)\right] \tag{16}$$

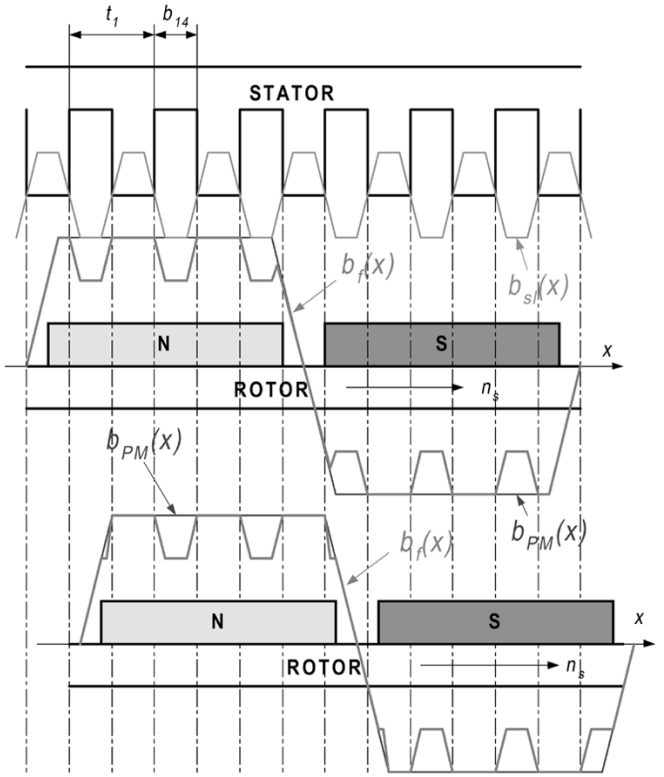

Fig. 2. Magnetic flux density waveforms in the air gap: $b_{PM}(x)$ excited by the rotor PMs, $b_{sl}(x)$ due to stator slots and $b_f(x)$—resultant. Only $b_{PM}(x)$ moves with the rotor.

where

$$I_1(X) = \int_{X+a}^{X+b} \left[-\frac{2\alpha}{k_C} AB^2 \sin\alpha x \cos^2\beta x\right] dx$$
$$= \frac{AB^2}{k_C}\left\{2\sin\left[\alpha\left(X+\frac{a+b}{2}\right)\right]\sin\left(\alpha\frac{a-b}{2}\right)\right.$$
$$+ \frac{\alpha}{\alpha+2\beta}\sin\left[(\alpha+2\beta)\left(X+\frac{a+b}{2}\right)\right]$$
$$\times \sin\left[(\alpha+2\beta)\left(\frac{a-b}{2}\right)\right]$$
$$+ \frac{\alpha}{\alpha-2\beta}\sin\left[(\alpha-2\beta)\left(X+\frac{a+b}{2}\right)\right]$$
$$\left.\times \sin\left[(\alpha-2\beta)\left(\frac{a-b}{2}\right)\right]\right\} \quad (17)$$

$$I_2(X) = \int_{X+a}^{X+b} \left[2\alpha A^2B^2 \sin\alpha x \cos\alpha x \cos^2 bx\right] dx$$
$$= A^2B^2\left\{\frac{1}{2}\sin\left[2\alpha\left(X+\frac{a+b}{2}\right)\right]\sin\left(\alpha(a-b)\right)\right.$$
$$+ \frac{\alpha}{4(\alpha+\beta)}\sin\left[2(\alpha+\beta)\left(X+\frac{a+b}{2}\right)\right]$$
$$\times \sin\left[(\alpha+\beta)(a-b)\right]$$
$$+ \frac{\alpha}{4(\alpha-\beta)}\sin\left[2(\alpha-\beta)\left(X+\frac{a+b}{2}\right)\right]$$
$$\left.\times \sin\left[(\alpha-\beta)(a-b)\right]\right\}. \quad (18)$$

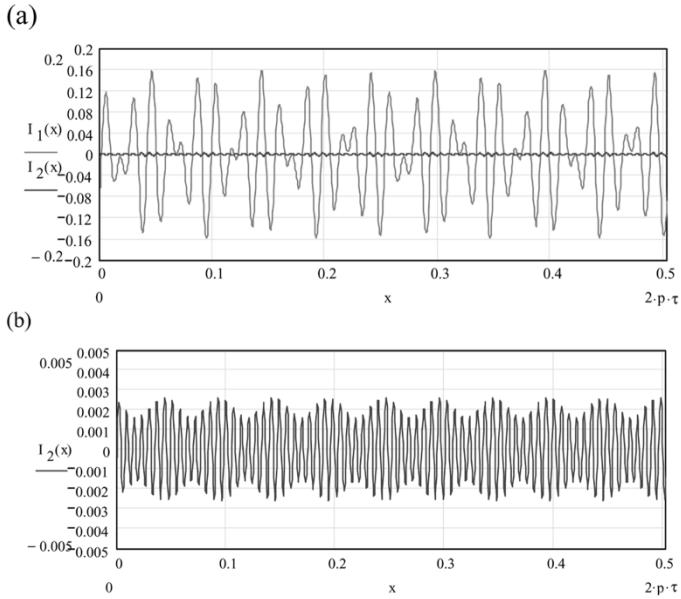

Fig. 3. Comparison of the first and second term in (16). (a) Integrals $I_1(X)$ and $I_2(X)$ according to (17) and (18). (b) Integral $I_2(X)$. Calculation results for a PMBM with embedded magnets, $s_1 = 36$ stator slots, $2p = 10$ poles, $g = 1$ mm, $L_i = 198$ mm, $t_1 = 14$ mm, $\tau = 50.3$ mm, $b_{14} = 3$ mm, $b_{fs} = 0$, $b_s = 14$ mm, $B_g = 0.76$ T, and $n_s = 11$ rev/s.

Since $I_1(X) \gg I_2(X)$, the following shorter form of cogging torque equation can be used

$$T_c(X) \approx -\frac{L_i g}{2\mu_0}\frac{D_{2\text{out}}}{2} I_1(X). \quad (19)$$

Fig. 3 clearly shows that the fundamental frequency of the cogging torque (first integral) is $f_c = s_1 n_s$, i.e., there are s_1 pulses per one revolution. The fundamental waveform is modulated by another waveform with frequency $f_{cp} = 2pn_s$, i.e., $2p$ pulses per revolution. The second integral indicates that there is negligible frequency $f_{c2} = 2s_1 n_s$, i.e., $2s_1$ pulses per revolution.

IV. Simplified Cogging Torque Equation

Putting $b_{PM}(x) = B_g$ in (11), the cogging torque will become a waveform with predominant frequency $f_c = s_1 n_s$ and constant amplitude. Such simplified equation which does not take into account the finite width of rotor poles has been derived in earlier publications of the author [11], [12]. For $b_{PM}(x) = B_g$, $\mu = 1$ and $k = 1$ the simplified cogging torque equation has the following form:

$$T_c(X) = -\frac{L_i g}{2\mu_0}\frac{D_{2\text{out}}}{2}\frac{d}{dX}\int_{X+a}^{X+b}\left[\frac{B_g}{k_C} - AB_g\cos\alpha x\right]^2 dx$$
$$= -\frac{L_i g}{2\mu_0}\frac{D_{2\text{out}}}{2}$$
$$\times \frac{d}{dX}\int_{X+a}^{X+b}\left[\left(\frac{B_g}{k_C}\right)^2 - \frac{2}{k_C}AB_g^2\cos\alpha x\right.$$
$$\left. + A^2B_g^2\cos^2\alpha x\right] dx$$
$$= -\frac{L_i g}{2\mu_0}\frac{D_{2\text{out}}}{2}\left[K_1(X) + K_2(X)\right] \quad (20)$$

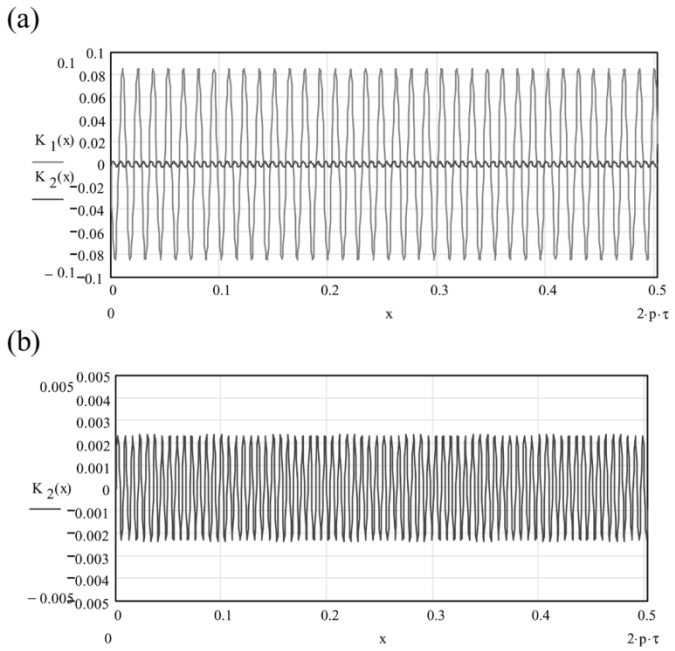

Fig. 4. Comparison of the first and second term in (20). (a) Integrals $K_1(X)$ and $K_2(X)$ according to (21) and (22). (b) Integral $K_2(X)$. Simulation has been done for a PMBM with the same parameters as specified in Fig. 3 caption.

where

$$K_1(X) = -\frac{4}{k_C} A B_g^2 \sin\left[\alpha\left(X + \frac{a+b}{2}\right)\right] \times \sin\left(\alpha \frac{a-b}{2}\right) \tag{21}$$

$$K_2(X) = A^2 B_g^2 \sin\left[2\alpha\left(X + \frac{a+b}{2}\right)\right] \times \sin\left[\alpha(a-b)\right]. \tag{22}$$

Since $K_1(X) \gg K_2(X)$ (Fig. 4), (20) can also be written in a shorter form

$$T_c(X) \approx -\frac{L_i g}{2\mu_0} \frac{D_{2\text{out}}}{2} K_1(X). \tag{23}$$

V. Influence of Ecentricity

The variation of the air gap for static eccentricity can be expressed analytically as [14]

$$g(x) = g\left[1 - \varepsilon \cos\left(\frac{\pi}{p\tau} x\right)\right] \tag{24}$$

where g is the mean air gap, $\epsilon = e/g$ is the relative eccentricity, and e is the displacement between the stator and rotor axis. Since the air gap is now the function of the x coordinate, the magnetic energy change depends on the variation of the air gap with the x coordinate. It is difficult to analyze (11) with the air gap $g(x)$ in the square bracket dependent on the x coordinate. It is more convenient to use the simplified (20) in which

$$A = 2\gamma \frac{g(x)}{t_1} k_{ok=1}^2 k_{sk=1}. \tag{25}$$

Thus,

$$\begin{aligned} T_c(X) &= -\frac{L_i g}{2\mu_0} \frac{D_{2\text{out}}}{2} \\ &\quad \times [K_1(X) + K_2(X) + K_3(X) \\ &\quad + K_4(X) + K_5(X)] \\ &\approx -\frac{L_i g}{2\mu_0} \frac{D_{2\text{out}}}{2} [K_1(X) + K_3(X)] \end{aligned} \tag{26}$$

where $K_1(X)$ and $K_2(X)$ are according to (21) and (22), respectively, and remaining terms are

$$\begin{aligned} K_3(X) &= 2\frac{1}{k_C} A B_g^2 \varepsilon \\ &\quad \times \left\{ \sin\left[(\theta+\alpha)\left(x + \frac{a+b}{2}\right)\right] \right. \\ &\quad \times \sin\left[(\theta+\alpha)\left(\frac{a-b}{2}\right)\right] \\ &\quad + \sin\left[(\theta-\alpha)\left(x + \frac{a+b}{2}\right)\right] \\ &\quad \left. \times \sin\left[(\theta-\alpha)\left(\frac{a-b}{2}\right)\right]\right\} \end{aligned} \tag{27}$$

$$\begin{aligned} K_4(X) &= -A^2 B_g^2 \varepsilon \\ &\quad \times \left\{ 2\sin\left[\theta\left(x + \frac{a+b}{2}\right)\right] \right. \\ &\quad \times \sin\left[\theta\left(\frac{a-b}{2}\right)\right] \\ &\quad + \sin\left[(\theta+2\alpha)\left(x + \frac{a+b}{2}\right)\right] \\ &\quad \times \sin\left[(\theta+2\alpha)\left(\frac{a-b}{2}\right)\right] \\ &\quad + \sin\left[(\theta-2\alpha)\left(x + \frac{a+b}{2}\right)\right] \\ &\quad \left. \times \sin\left[(\theta-2\alpha)\left(\frac{a-b}{2}\right)\right]\right\} \end{aligned} \tag{28}$$

$$\begin{aligned} K_5(X) &= A^2 B_g^2 \varepsilon^2 \\ &\quad \times \left\{ \frac{1}{4}\sin\left[2(\theta+\alpha)\left(x + \frac{a+b}{2}\right)\right] \right. \\ &\quad \times \sin\left[(\theta+\alpha)(a-b)\right] \\ &\quad + \frac{1}{4}\sin\left[2(\theta-\alpha)\left(x + \frac{a+b}{2}\right)\right] \\ &\quad \times \sin\left[(\theta-\alpha)(a-b)\right] \\ &\quad + \frac{1}{2}\sin\left[2\gamma\left(x + \frac{a+b}{2}\right)\right] \sin\left[\gamma(a-b)\right] \\ &\quad + \frac{1}{2}\sin\left[2\alpha\left(x + \frac{a+b}{2}\right)\right] \\ &\quad \left. \times \sin\left[\alpha(a-b)\right]\right\}. \end{aligned} \tag{29}$$

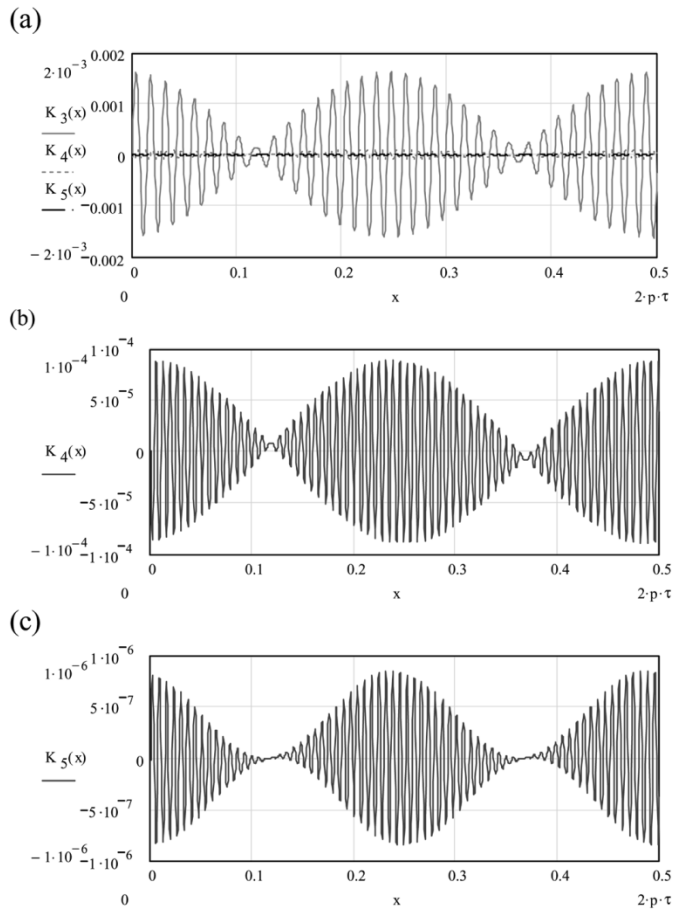

Fig. 5. Comparison of the third, fourth and fifth terms in (26). (a) Integrals $K_3(X)$, $K_4(X)$, and $K_5(X)$ according to (27)–(29). (b) Integral $K_4(X)$. (c) integral $K_5(X)$. Simulation has been done for a PMBM with the same parameters as specified in Fig. 3 caption and relative eccentricity $\varepsilon \approx 0.2$.

Fig. 5 shows that $K_3(X) \gg K_4(X)$ and $K_3(X) \gg K_5(X)$. Including the finite width of poles the cogging torque equation can eventually be

$$\begin{aligned} T_c(X) = &-\frac{L_i g}{2\mu_0}\frac{D_{2\text{out}}}{2} \\ &\times [I_1(X) + I_2(X) + K_3(X) \\ &+ K_4(X) + K_5(X)] \\ \approx &-\frac{L_i g}{2\mu_0}\frac{D_{2\text{out}}}{2}\left[I_1(X) + K_3(X)\right]. \end{aligned} \tag{30}$$

VI. Calculations and Comparison With Measurements

The results of analytical calculation of the cogging torque according to (16) which includes the finite width of the rotor magnet are shown in Fig. 6(a) while the results of calculations according to simplified equation (20) are shown in Fig. 6(b). The calculated and measured cogging torque produced by the same motor ($2p = 10, s_1 = 36$) and the same air-gap magnetic flux density $B_g = 0.76$ T is shown in Fig. 7. To capture the cogging torque pulsations, a torque transducer, oscilloscope, and data acquisition system have been used. The test results and computation results have been written to an Excel file. It can be seen that the measured cogging torque waveform is

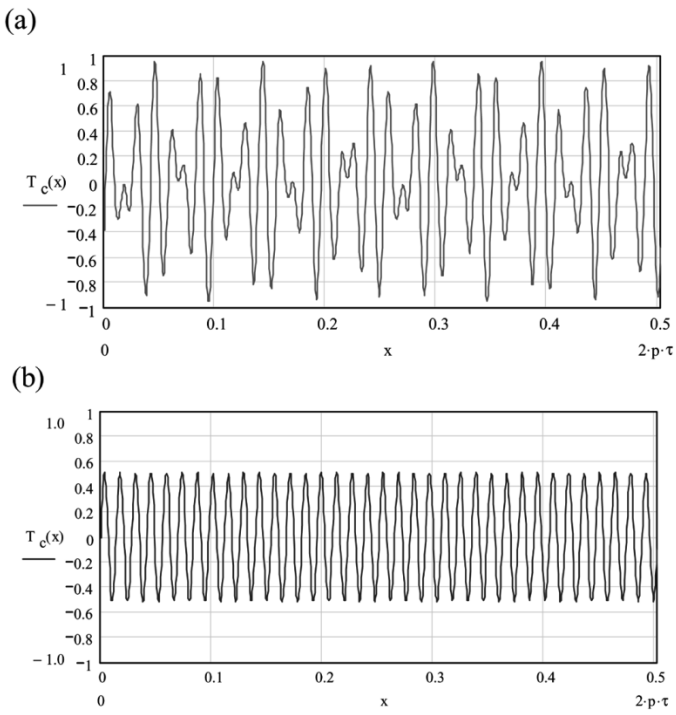

Fig. 6. Cogging torque calculation results (N·m versus meter): (a) according to (16). (b) According to (20). Design data of the PMBM are the same as specified in Fig. 3 caption, relative eccentricity $\varepsilon \approx 0.2$.

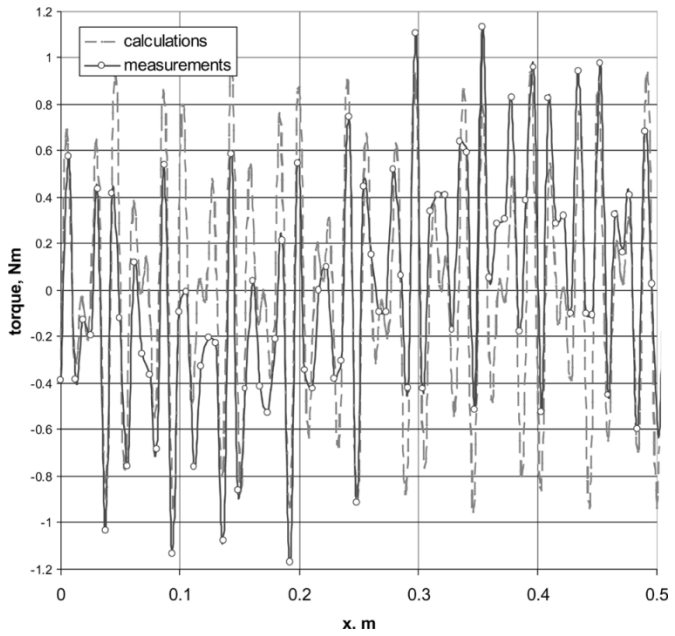

Fig. 7. Comparison of calculated cogging torque according to (30) and measured cogging torque for one full rotor revolution. Design data of the PMBM are the same as specified in Fig. 3 caption, relative eccentricity $\varepsilon \approx 0.2$.

modulated by a sinusoid with the period equal to one revolution $2p\tau$, ie.,

$$K(x) = -M \sin\left(\frac{\pi}{p\tau}x\right). \tag{31}$$

This effect is due to the misalignment of the rotor and transducer shafts. The small shaft misalignment is difficult to avoid. The constant M in (31) is proportional to the degree of misalignment.

VII. Conclusion

In comparison with the finite-element method (FEM), the presented analytical method gives immediate results and allows for fast analysis of different magnetic circuit geometries of PM brushless motors.

It can easily be implemented in the design procedure of commercial PM brushless motors and new products. Equation (16) can capture the effect of the finite width of PMs while simplified equation (20) can only predict the fundamental frequency of the cogging torque and approximately its amplitude. Equation (20) can only be recommended for two-pole machines with large pole shoe-to-pole pitch ratio $\alpha_i \geq 0.9$. The effect of eccentricity is included by $K_3(x)$, $K_4(x)$, and $K_5(x)$ and can be predicted with the aid of (26). For the detailed study of the cogging torque the best results can be obtained using (30).

There is a certain discrepancy between the analytical prediction and measurements caused by the misalignment of the rotor and torque transducer shafts. On the other hand, cogging torque measurements are difficult and the high accuracy of measurements is always questionable.

Appendix I

A. Influence of Stator Slots on Magnetic Field Distribution

The magnetic flux density distribution in the air gap of a PM machine can be analyzed in a similar way as that of an induction machine with slotted stator and smooth rotor [7], [14]. The normal component of the magnetic flux density in the air gap is a sum of the mean flux density $b_{\text{mean}}(x)$ and periodical component with the period equal to the slot pitch t_1, i.e.,

$$b_f(x) = b_{\text{mean}}(x) + \sum_k B_k \cos\left(k\frac{2\pi}{t_1}\right) \tag{32}$$

where [7], [14]

$$b_{\text{mean}}(x) = \frac{B_0}{k_C}. \tag{33}$$

Considering the air-gap magnetic field distribution only in the interval of one pole pitch τ, the flux density $B_0 = B_g$ where B_g is the flat-topped value of the magnetic flux density in the air gap. Fourier series coefficient B_k in (32) depends on the approximation of the magnetic flux density distribution and for skewed slots can take the form

$$B_k = -2\gamma\frac{g}{t_1}B_0 k_{ok}^2 k_{sk}^2. \tag{34}$$

Carter coefficient k_C is expressed using the following well-known equation [14]:

$$k_C = \frac{t_1}{t_1 - \gamma g} \tag{35}$$

$$\gamma = \frac{4}{\pi}\left[\frac{b_{14}}{2g}\arctan\left(\frac{b_{14}}{2g}\right) - \ln\sqrt{1+\left(\frac{b_{14}}{2g}\right)^2}\right]. \tag{36}$$

Thus, (32) can be brought to the form

$$b_f(x) = B_0\left[\frac{1}{k_C} - 2\gamma\frac{g}{t_1}\sum_{k=1}^{\infty} k_{ok}^2 k_{sk}^2 \cos\left(k\frac{2\pi}{t_1}x\right)\right]. \tag{37}$$

In order to include the influence of the finite width of PMs or pole shoes on the cogging effect, the flux density B_0 must be expressed as a periodic function of the pole pitch τ, i.e., $B_0 = b_{PM}(x)$, where $b_{PM}(x)$ is according to (2).

Appendix II

A. Magnetic Flux Density Excited by PMs

Equation (2) describes the distribution of the normal component of the magnetic flux density excited by PMs (slotless machine) for $B_0 = b_{PM}(x)$. For periodic variation of the PM flux density

$$b_f(x) = \sum_\mu B_g b_\mu k_{s\mu}\cos\left(\mu\frac{\pi}{\tau}x\right) \times\left[\frac{1}{k_C} - 2\gamma\frac{g}{t_1}\sum_{k=1}^{\infty} k_{ok}^2 k_{sk}^2\cos\left(k\frac{2\pi}{t_1}x\right)\right]. \tag{38}$$

The coefficient of Fourier series $b\mu$ for higher space harmonics $\mu = 6l \pm 1$ in (2) depends on the shape of the normal component of the magnetic flux density distribution in the air gap. According to the author, it can be expressed as [11]

$$\begin{aligned} b_\mu = \frac{4}{\tau}\Bigg[&\left[\frac{c_p}{c_p^2 + \left(\mu\frac{\pi}{\tau}\right)^2}\sinh(\alpha_p) - 6\left(\frac{\tau}{\mu\pi}\right)^4\frac{1}{b_t^3}\cosh(\alpha_p)\right] \\ &+3\left(\frac{\tau}{\mu\pi}\right)^2\frac{2}{\tau - b_p}\cosh(\alpha_p)\Bigg] \\ &\times\sin\left(\mu\frac{\pi}{2}\right)\sin\left(\mu\frac{\pi b_t}{\tau}\right) \\ &+\frac{4}{\tau}\left[\frac{\mu\frac{\pi}{\tau}}{c_p^2 + \left(\mu\frac{\pi}{\tau}\right)^2} + 6\left(\frac{\tau}{\mu\pi}\right)^3\frac{1}{b_t^2} - \frac{\tau}{\mu\pi}\right] \\ &\times\cosh(\alpha_p)\sin\left(\mu\frac{\pi}{2}\right)\cosh\left(\mu\frac{\pi b_t}{\tau}\right) \end{aligned} \tag{39}$$

where

$$b_p = \alpha_i\tau; \quad c_p = 2\frac{\alpha_p}{b_p} \quad b_t = \frac{\tau - b_p}{2}. \tag{40}$$

The pole width b_p-to-pole pitch τ ratio for PM brushless motors $\alpha_i = b_p/\tau = 0.65$–$0.92$. The parameter α_p describes the shape of the magnetic flux density waveform under the PM or pole shoe. For a constant (flat-topped) value of the magnetic flux density in the range $-0.5b_p \leq x \leq 0.5b_p$ as in Fig. 1 the parameter $\alpha_p = 0$. For the magnetic flux density curve changing underneath the pole according to hyperbolic cosine law (concave curve) the parameter $0 < \alpha_p \leq 1$.

References

[1] B. Ackermann, J. H. H. Janssen, and R. Sottek, "New technique for reducing cogging torque in a class of brushless d.c. motors," *Proc. Inst. Elect. Eng.*, pt. B, vol. 139, no. 4, pp. 315–320, 1992.

[2] N. Bianchi and S. Bolognani, "Design techniques for reducing the cogging torque in surface mounted PM motors," *IEEE Trans.Ind. Applicat.*, vol. 36, pp. 1259–1265, Sept./Oct. 2002.

[3] C. Breton, J. Bartolome, J. A. Benito, G. Tassinario, I. Flotats, C. W. Lu, and B. J. Chalmers, "Influence of machine symmetry on reduction of cogging torque in permanent magnet brushless motors," *IEEE Trans. Magn.*, vol. 36, pp. 3819–3823, Sept. 2000.

[4] W. Cai, D. Fulton, and K. Reichert, "Design of permanent magnet motors with low torque ripple," in *Proc. Int. Conf. Electric Machines(ICEM'00)*, vol. 3, Espoo, Finland, 2000, pp. 1384–1388.
[5] S. X. Chen, T. S. Low, H. Lin, and Z. J. Liu, "Design trends of spindle motors for high performance hard disk drives," *IEEE Trans. Magn.*, vol. 32, pp. 3848–3850, Sept. 1996.
[6] J. de La Ree and N. Boules, "Torque production in permanent magnet synchronous motors," *IEEE Trans. IA*, vol. 25, no. 1, pp. 107–112, 1989.
[7] M. Dabrowski, *Magnetic Fields and Circuits of Electrical Machines* (in Polish). Warsaw, Poland: WNT, 1971.
[8] J. R. P. Deodhar, D. A. Staton, T. M. Jahns, and T. J. E. Miller, "Prediction of cogging torque using the flux-MMF diagram technique," *IEEE Trans. Ind. Applicat.*, vol. 32, pp. 569–576, May/June 1996.
[9] L. Dreyfus, "Die Theorie des Drehstrommotors mit Kurzschlussanker," Ingeniörsvetenkapsakademiens, Stockholm, Sweden, pp. 1–47, 1924.
[10] J. F. Gieras, "Electrodynamic levitation forces—Theory and small-scale results," *Acta Tech. CSAV*, no. 4, pp. 389–413, 1981.
[11] J. F. Gieras and M. Wing, *Permanent Magnet Motors Technology: Design and Applications*, 2nd ed. New York: Marcel Dekker, 2002.
[12] J. F. Gieras and M. E. Marler, "Analytical prediction of torque ripple in permanent magnet brushless motors," in *Proc. Int. Conf. Electric Machines (ICEM'02)*, Brugge, Belgium, 2002, pp. 33–34.
[13] D. C. Hanselman, "Effect of skew, pole count and slot count on brushless motor radial force, cogging torque and back EMF," *Proc. Inst. Elect. Eng.*, pt. B, vol. 144, no. 5, pp. 325–330, 1997.
[14] B. Heller and V. Hamata, *Harmonic Field Effects in Induction Machines*. Prague, Czechoslovakia: Academia, 1977.
[15] Z. Q. Zhu and D. Howe, "Analytical prediction of the cogging torque in radial field permanent magnet brushless motors," *IEEE Trans. Magn.*, vol. 28, pp. 1371–1374, Mar. 1992.
[16] ——, "Influence of design parameters on cogging torque in permanent magnet machines," *IEEE Trans. Energy Conversion*, vol. 15, pp. 407–412, Dec. 2000.

Jacek F. Gieras (M'84–SM'88–F'02) received the M.Eng. degree with distinction from the Technical University of Łodz, Łodz, Poland, in 1971, and the Ph.D. degree in power electrical engineering (electrical machines) and the Dr hab. degree in electrical engineering (electromagnetic field theory) from the University of Technology, Poznan, Poland, in 1975 and 1980, respectively.

From 1971 to 1998, he pursued his academic career at several universities worldwide, including Poland, Canada, Jordan, and South Africa. He was also a Central Japan Railway Company Visiting Professor at The University of Tokyo (Endowed Chair in Transportation Systems Engineering), Tokyo, Japan, Guest Professor at Chungbuk National University, Choengju, Koreea, and Visiting Professor at the University of Rome "La Sapienza," Rome, Italy. In 1987, he was promoted to the rank of Full Professor (life title given by the President of the Republic of Poland). Since 1998, he has been involved in industry-oriented research and innovations at the United Technologies Research Center, East Hartford, CT. He has authored or coauthored seven books, over 200 scientific and technical papers, and ten patents. His most important books of international standing are *Linear Induction Motors* (London, U.K.: Oxford Univ. Press, 1994), *Permanent Magnet Motors Technology: Design and Applications* (New York: Marcel Dekker, 1996, 2nd ed. 2002) (coauthor M. Wing), *Linear Synchronous Motors: Transportation and Automation Systems* (Boca Raton, FL: CRC Press, 1999), and *Axial Flux Permanent Magnet Machines* (Boston–Dordrecht–London: Kluwer, 2004) (coauthors R. Wang and M. Kamper).

Prof. Gieras is a member of numerous steering committees of international conferences and is cited by several of Marquis *Who's Who* publications.